Highly Informed Robotic 3D Printed Polygon Mesh

A Novel Strategy of 3D Spatial Printing

Lei Yu
Tsinghua University

Yijiang Huang
University of Science and Technology of China

Zhongyuan Liu

Sai Xiao
Archi-solution Workshop (Beijing)

Ligang Liu

Guoxian Song
University of Science and Technology of China

Yanxin Wang
Archi-solution Workshop (Beijing)

1

ABSTRACT

Though robotic 3D printing technology is currently undergoing rapid development, most of the research and experiments are still based on a bottom up layering process. This paper addresses long term research into a robotic 3D printed polygon mesh whose struts are directly built up and joined together as rapidly generated physical wireframes. This paper presents a novel "multi-threaded" robotic extruder, as well as a technical strategy to create a "printable" polygon mesh that is collision-free during robotic operation. Compared to standard 3D printing, architectural applications demand much larger dimensions at human scale, geometrically lower resolution and faster production speed. Taking these features into consideration, 3D printed frameworks have huge potential in the building industry by combining robot arm technology together with FDM 3D printing technology. Currently, this methodology of rapid prototyping could potentially be applied on pre-fabricated building components, especially ones with uniform parabolic features. Owing to the mechanical features of the robot arm, the most crucial challenge of this research is the consistency of non-stop automated control. Here, an algorithm is employed not only to predict and solve problems, but also to optimize for a highly efficient construction process in coordination of the robotic 3D printing system. Since every stroke of the wireframe contains many parameters and calculations in order to reflect its native organization and structure, this robotic 3D printing process requires processing an intensive amount of data in the back stage.

3D PRINTED FRAMEWORK

A polygon mesh is often known as a collection of vertices, edges and faces that define the shape of a polyhedral object in 3D computer graphics and solid modeling. Typical 3D printing techniques slice the polygon mesh with evenly spaced horizontal planes and rebuild the model through the layering of contour crafted slices. But this method of fabrication is too slow to satisfy the scale of production for the building industry. When Solid Doodler came out a few years ago, its spatial thermoplastic extrusion drew much attention. Especially with its powerful and flexible maneuvering that could potentially simulate the performance of a human arm, the industrial robot arm has proven to be a perfect choice for the task.

Several research teams have had tremendous achievements in spatial 3D printing by robot arms, for instance, Freeform Printing (Oxman et al. 2013), Iridescence Print (Helm et al. 2015), 'TN-01' by Branch Technology, and Mesh Mold (Norman et al.2015, Figure 2). These precursors mainly use a 6-axis industrial robot mounted with an FDM extruder as the end effector to produce a matrix of wireframes. The outputs could either be used as a mesh mold that is an alternative to conventional formwork or as a self-supporting structure. The features of the framework evoke a truss system that extends beyond the traditional notion of polygon mesh that is only defined by geometric surfaces.

All the projects above share certain common characteristics as the construction processes are all based on a layering process from the ground up. The nature of the process would result in the following shortcomings:

- The polygon mesh is rebuilt after being sliced into layers with a certain thickness, which in turn causes loss of geometric detail and resolution.
- These layers are different from the typical 3D printing thin slices, but no more than the thicken "strata" composed with triangle strut groups that are seen in the example above.
- The inherent weakness between the layers in a structure fabricated through the contouring process could cause fractures between layers when the structure is under abrupt force and loads. Thus this feature would render the process improper for fabrication of large-scale building components that require additional infill.

Based on the current research of robotic 3D printing, there are three potential aspects that are worth investigation.

- How to maintain a proper resolution of the original mesh in the definition used for physical output.

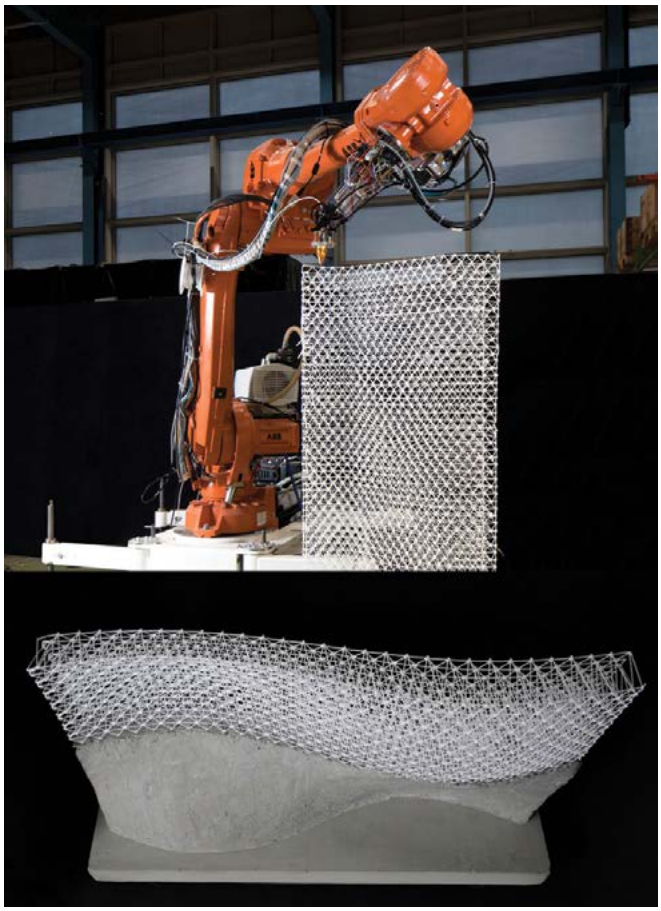

2

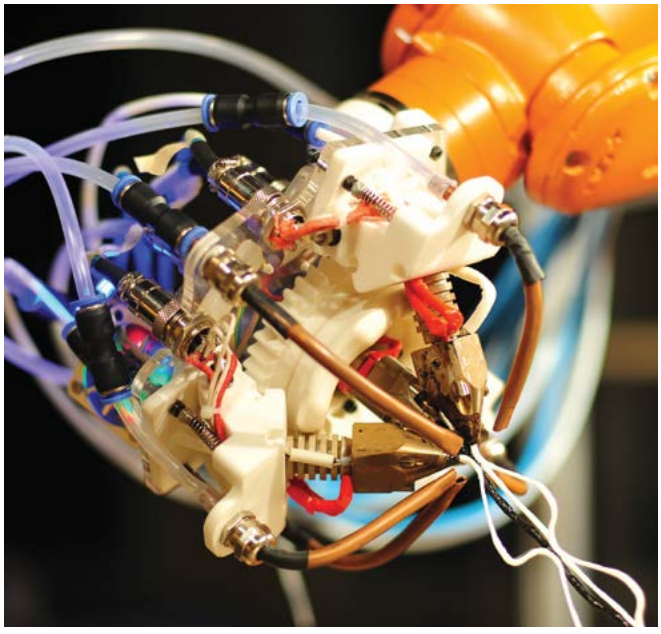

3

2 Mesh Mould by Norman Hack and Willi Viktor Lauer.

3 Hyperbolic Extruder on Robot, a 2014 Workshop in School of Architecture and Urban Planning, Tongji University, Shanghai China.

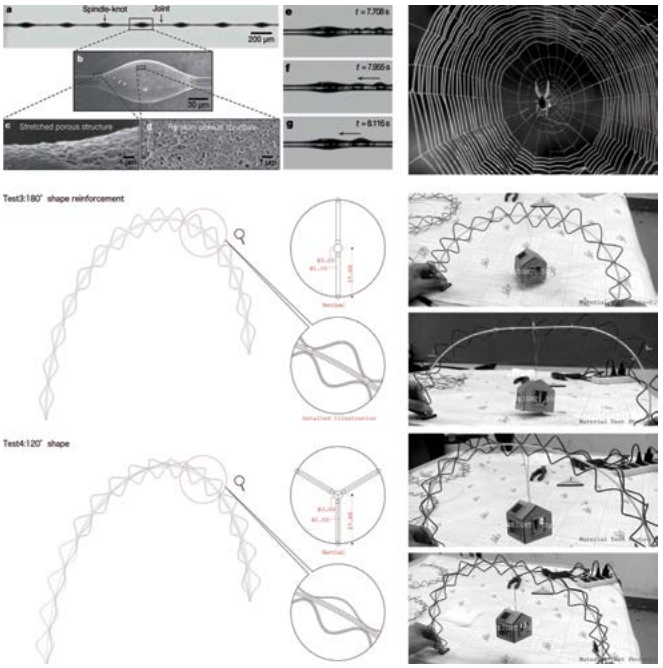

4

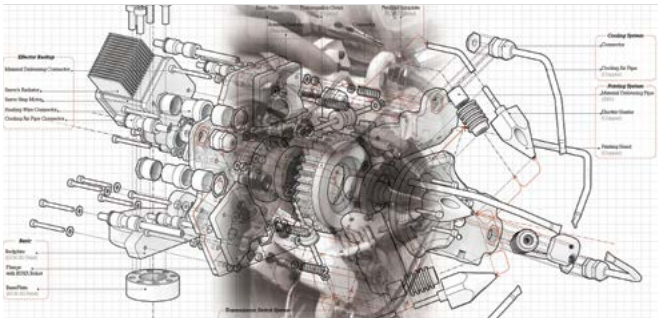

5

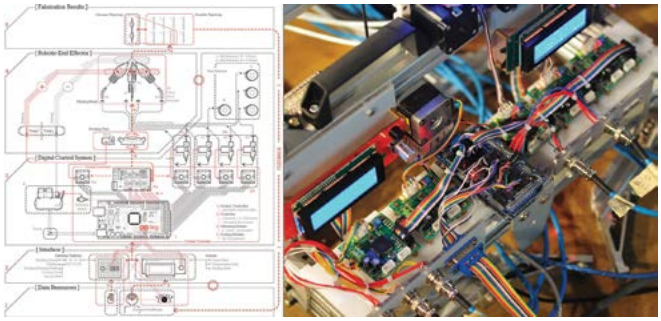

6

- How to utilize the potential of the robot arm's dexterity which is much more flexible than the generic 3D printing CNC machine.
- How to take advantage of the geometrical features of the original polygon mesh to generate a 3D spatial wireframe and reinforce its strength in all directions.

ROBOTIC 3D SPATIAL PRINTED POLYGON MESH

In the past two years, we have dedicated a constant effort on how to employ an industrial robot arm in the rapid construction of frameworks. This combination has shown great potential that could fundamentally alter the conventional method of concrete mold-work, which has always faced criticism for overly high cost and being labor intensive, especially for customized building parts. Our research focuses on a novel direction that mesh framework could be strategically 3D printed according to its native topographies. The key focus of the research is the spatial configuration of the 3D printing process and its strength, with particular attention to the span, deformation, connection and generation sequence. It contains two stages that involve different attitudes toward material configuration. The former is based on multi-threaded extrusion, while the latter is single-threaded extrusion.

Multi-threaded Extrusion and Form Definition

The goal of this research stage is to create standalone lineal overhang, which is capable of rising up as a self-supporting structure. In order to increase the thin plastic filament's capacity for a larger span, this research concentrated heavily on the design of the robot arm's end effector, which could produce significant composite extrusions embedded with more structural freedom.

Spider silk was investigated under a microscope for more evidence. We were surprised to discover that the profile of spider silk appears as a series of spindle knots joined together under the microscope at 200 μm. After a few tests with hand-made models lifting the same block, including a model of one center tread surrounded by two or three corrugated ABS filaments (Figure 3&4), we discovered a model that is highly efficient in increasing toughness of the extrusion through the spatial configurations. Design decisions for the robot's 'hand' were based on creating these regulating knots along the motion path of the robot. There are four nozzles required for this mechanism. One center nozzle extruding a fat straight thread, and the other three outer nozzles generating undulating curves that meet periodically with the center thread (Figure 5). The outer nozzles are fixed onto a sweeping mechanism driven by stepper motors to ensure their open-close movements. Extruder and robot arm are synchronized by an Arduino system (Figure 6). There are many essential driving parameters, such as the robot effector's moving speed, extruding speeds, rotation speed of the center sweeper, nozzle temperature etc. All of the parameters need to be coordinated in order to create a smooth lineal profile similar to the hand-made test model.

The robotic 3D printer generates a hyperbolic curve that addresses extra geometric and structural challenges (Figure 7).

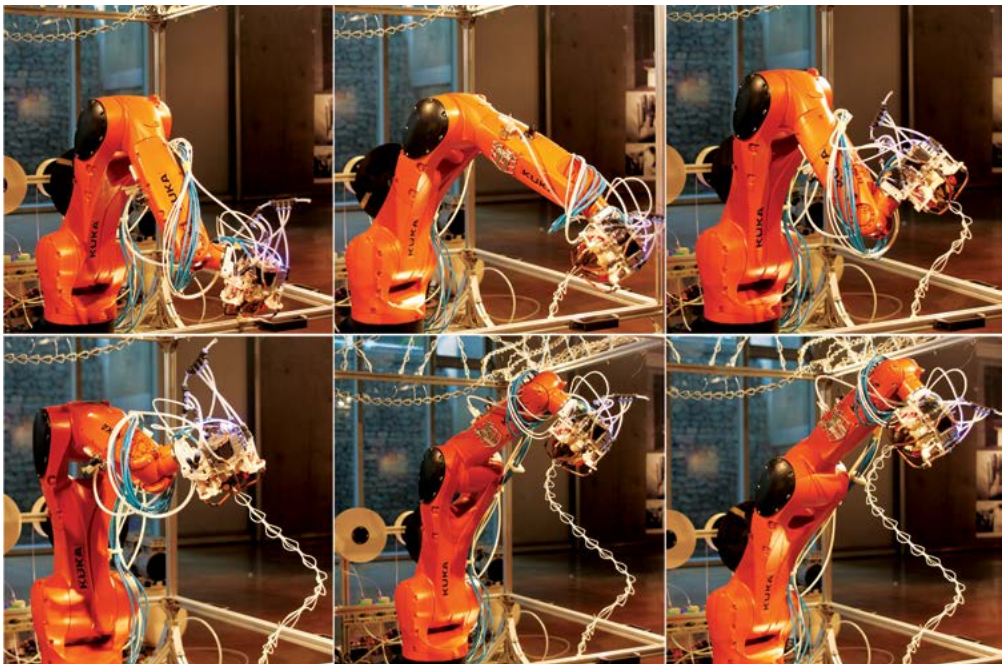

7

4 Spider Silk Macro Pictures and Simulating Test.

5 Robot End Effector Design and Assembly.

6 Arduino Control System to synchronize 5 stepper motors with 6 axis industrial robot.

7 Process of Hyperbolic Extrusion.

Unlike the arch model with two anchor points, this hyperbolic helix has only one standing point while supporting itself by its own rigidity derived from its biomimetic configuration. We are also aware that the ABS filament, a common thermo-plastic, has a significant shrinkage rate, which means that after the melted plastic extrusion cools down, the shape will deform slightly, which could cause joint dispositions under some circumstances. Even though the multi-threaded extrusion gains certain achievement with its attractive performance,three main concerns drive the research into the second stage – a massive structural frame:

- Deformation due to material shrinkage and gravity will cause joints to dislocate from the adjacent connecting struts.
- The hyperbolic configuration is hard to connect with other components other without extra supports.
- The multi-threaded robot end effector is too big to avoid collision with the existing 3D printed elements, and always causes the robot to run out of working range.

Single-threaded Extrusion and Form Definition

From the previous study, we have come to a conclusion that in order to achieve a better-defined 3D printed mesh, the robot effector should be as small as possible for the process to be collision free. Therefore, we started to reconsider single-threaded extrusion. Even though we abandoned the multi-threaded extrusion approach, much of the experience and parameters are were transferred into the next stage.

Industry robots have inborn constraints which have to be considered at each step of motion to plan a valid working path. The constraints of motion planning include existing obstacles in the working space, limits from articulated singularities and articulated robot joint angles. According to the American National Standard for Industrial Robots and Robot Systems, singularity is defined as a condition caused by the collinear alignment of two or more robot axes resulting in unpredictable robot motion and velocities.

Singularities occur as:

- Wrist singularities: occur when the axes of Joints 4 and 6 are aligned;
- Alignment singularities: occur when Joint 6 (wrist) and Joint 1 axes are aligned;
- Elbow singularities: occur when the arm is fully extended. In this case, as the elbow joint becomes further extended, higher joint speeds are required to maintain constant Cartesian speed. The robot cannot extend beyond its reach.

These constraints affect a tiling style construction process much less than an 'orientation style' construction technique, which is the method involved in this paper. If the effector's orientation and the space angle of mesh edges are to be matched within a certain angle for making straight and strong struts, there are many more parameters that need to be systematically managed. The data requires careful calculation and simulation for validation and optimization beforehand, testing for any possibility of halting during fabrication.

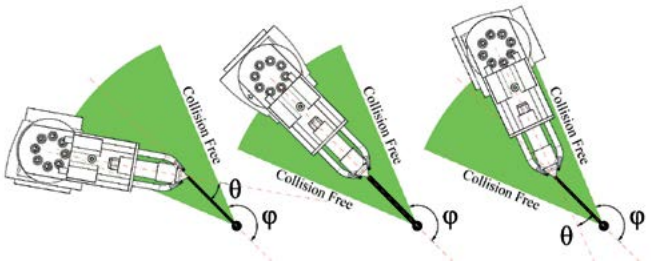

8

9

10

8 Diagrams of Nozzle Orientation, Thermoplastic Aggregation and Collision Free zone.

9 Process of One Single Extrusion.

10 Relationship of Working Angles.

The mechanism of the robot end effector design and the proper algorithm are both key elements to this research that rigorously rely on each other. First of all, the cone volume of the extruding effector should be sharp enough on angle α (Figure 8) to avoid collision with existing static obstacles. Furthermore, only when angle θ is limited within a certain degree will the extruded thermoplastic be aggregated into a straight line(-Figure 9). However, the cone volume of the heating block has to contain a heater, heating nozzle, dual cooling nozzles and a thermistor. All these necessary parts together force the cone to be above a certain volume in size. On the other hand, each spatial stroke has to consider its neighborhood condition so that it will not touch or collapse onto its adjacent parts. This process requires the management of the φ angles. On the top of these two considerations, the sequence that the mesh edges are built needs to be specified, where every step of operation from the first edge to the last one is ensured to be valid regarding these hard and soft constraints.

The Collision Area (Figure 10) illustrates the virtual working zone, which tightly relates to a few angles that contribute to the development of the mesh construction sequence and avoid the singularities of robot. The process of pursuing this magical zone consists of three steps that almost entirely depend on the algorithm.

- Rebuild mesh polygon: explode mesh into edges and reorganize them in an adaptable queue for robotic 3D spatial printing.
- Validation of the rebuilt mesh: each re-connection has to be qualified not only to avoiding the existing printed struts, but also to be responsible for the construction of the remaining mesh edges which will be potentially influenced by the former process.
- Validation of robot control: singularity or self-lock cases need to be entirely removed in the whole motion planning to avoid accidental disruption to the fabrication process.

The algorithm is meticulously driven by this comprehensive solution. Compared to the generic tiling 3D printing method, this method has to be pre-calculated repetitively to guarantee the correct joint-to-joint plastic extrusion and the fluency of the overall fabrication process. Therefore, each stroke has a set of information including both the basic point XYZ positions and their spatial vectors. This process generates a massive amount of data. The data is filtered, optimized and organized into the most appropriate groups, becoming the data package to drive the actual working path.

Re-composition of Polygon Mesh

The reason the Stanford Bunny (Figure 11) was selected as the test object is that this typical case of computer graphics bears most of the geometrical features of a polygon mesh. The result of the test could potentially be applied within the construction of most architecture forms.

To reduce the calculation, the edges of the polygon mesh are sorted into different groups based on their geometrical features. As in the Stanford Bunny, the portion of the ear color coded red and the top skull portion in colored in green represent grouped sub-entities. Then each sub-entity is calculated for sequence configuration separately. In this way, each edge's fabrication data only needs to be considered and validated within a smaller set instead of the whole. Even though it still performs like the

layering concept in a certain sense, this sub-entities concept results in a much larger volumetric structure than flat slices. This methodology takes not only point-to-point definition into consideration, but also point-to-point orientation.

Specifically, the strut set S is decomposed into two layers, B and T, each time, where T is the top layer and B the bottom layer. The decomposition methodology has to guarantee that:

- The size of upper part T is small enough so that the sequence-searching algorithm can be applied efficiently within the capacity of the computer.
- The lower part B is in a structurally stable state, i.e. each node has limited deformation so that the robot can locate it in the subsequent printing process.

The decomposition algorithm can be recursively applied on the lower part B until the termination criteria are satisfied.

Physical constraint: At any intermediate fabrication state, the fabricated frame shape should keep stable with limited deformation for each node. Thus, for the deformation vector:

$$||d_i^{\text{transf}}|| < \epsilon, \qquad \text{where } i = 1, 2, ..., N \tag{1}$$

Before introducing the optimized model, we will define the notations that are used. As the basic fabrication element in this solution is the strut, layer decomposition divides the set of frame strut ε into two strut sets every time, or in mathematical context, finds a cut on ε. The division has the relation of ε = BUT, where B and T share common nodes. If strut e_i and e_j share one common node, we then say they are connected, and then define the weight between them as w_{ij}. Thus, the cut would be:

$$w(S,T) = \sum_{e_i \in B, e_j \in T} w_{ij} \tag{2}$$

Optimization model: The objective of the layer decomposition is to limit the size of the upper part S. The constraint is that the lower part must have limited deformation. We need to verify the constraint by confirming the deformation vector computed by the stiffness equation (Hughes 2012, Kassimali 2012) satisfies the physical constraint. To achieve this goal, we define a weight graph on the current frame structure. The aim of the optimization model is to find a minimum cut on the weighted graph with a stable constraint:

$$\begin{aligned} &\min_{\mathcal{B},\mathcal{T}} \ w(\mathcal{B},\mathcal{T}) \\ &\text{s.t. } \mathbf{K}(\mathcal{B})\mathbf{d}(\mathcal{B}) = \mathbf{f}(B), \\ &\quad \|\mathbf{d}_i^t(\mathcal{B})\|_2 < \varepsilon, \\ &\quad S^t \subset \mathcal{T}, \\ &\quad S^b \subset \mathcal{B}, \end{aligned} \tag{3}$$

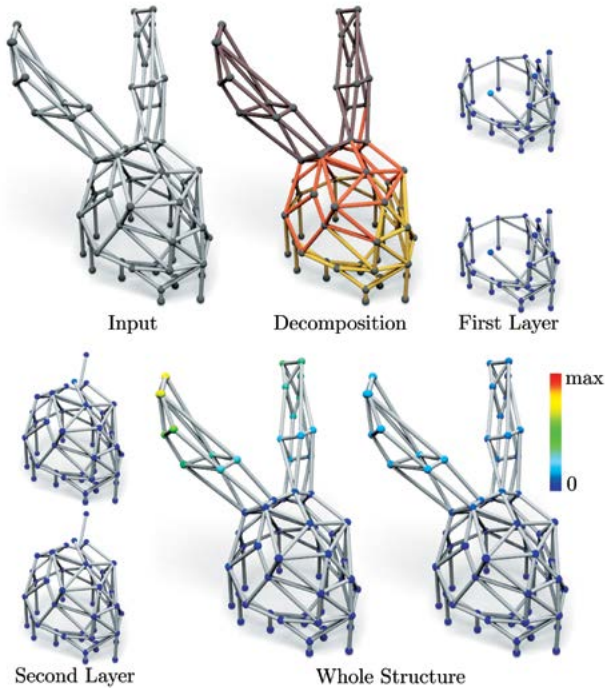

11

Algorithm 1: Layer Decomposition Algorithm

```
while |T| >tolerance for sub-part size do
    G = T;
    Define the weight w_ij according to Equation (4);
    Construct stiffness matrix;
    Set boundary value;
    iter = 0;
    while Reweighing termination criteria = False do
        ADMM solver;
        Update reweighting factor;
        iter = iter+1;
    if Solution is feasible then
        Cut G into Set T and B according to the computation result;
    else
        Return False (no feasible decomposition can be found);
```

12

Algorithm 2: SequenceSearching(k, s_{i_k})

```
Add s_{i_k} into the printed strut set;
Delete s_{i_k} from the unprinted strut set;
while candidate set is not empty do
    Set the strut s' with the minimal cost E(s') as s_{i_{k+1}};
    if SequenceSearching(k+1, s_{i_{k+1}}) = True then
        Print strut s_{i_{k+1}};
        Return True;
    else
        Delete s' from the candidate set;
if Candidate Set is not empty then
    Return True;
else
    Return False;
```

13

11 Polygon Mesh Decomposition in Grouped Layer.

12 Algorithm 1: Layer Decomposition.

13 Algorithm 2: Sequence Searching.

Algorithm 3: Fabrication sequence design (overall)

```
Input frame shape G is decomposed into layers of G_1, ..., G_L by
  iteratively applying Algorithm 2;
for each layer G_l do
    if SequenceSearching(1, s_i1) = False then
        Return False (No valid printing sequence found);
Return True (a valid fabrication sequence is obtained);
```

14

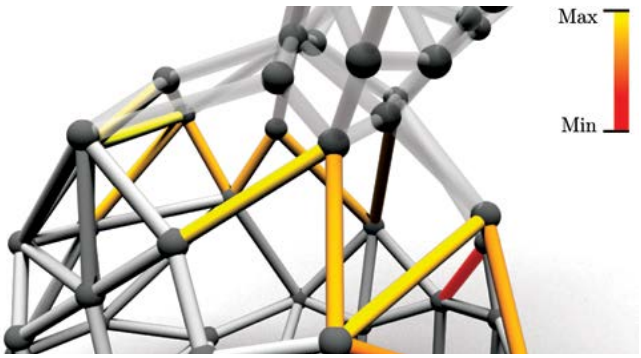

15

14 Algorithm 3 for Fabrication Sequence Design.

15 Extruding Sequence Probing Simulation.

Here S^t and S^b are respectively the top and bottom boundary struts of the input wireframe. K is the stiffness matrix of sub-structure *B* and *f* is the gravity force associated with the bending moment of the nodes (Hughes 2012, Kassimali 2012). To make the size of set S small, the cut should be close to the top boundary. To achieve this purpose, we define weight w_{ij} as:

$$w_{ij} = \begin{cases} exp(-\beta h^2(v_k)), & e_i \text{ and } e_j \text{ share node } v_k \\ 0, & \text{otherwise.} \end{cases} \quad (4)$$

Here, parameter β is used to control the weight distribution and $h^2(vk)$ is the normalized height of the node *vk*. In this way, the weights of the nodes close to the top boundary are small, which makes the cut boundary as high as possible and thus the top sub-part T is as small as possible.

Numerical computation of the decomposition algorithm: This is a constrained discrete optimization problem. We first simplify the binary optimization problem into a continuous optimization problem and then use an iterative re-weighting scheme (Lai et al. 2013) to solve this constrained optimization problem. In each iteration re-weighing loops, we adopt the Alternating Direction Method of Multipliers (ADMM) (Boyd et al. 2011) to solve sub-problems, as shown in Algorithm 1 (Figure 12).

Fabrication Sequence Finding

Collision is the most critical concern in this phase of the fabrication sequence. Quite different from the tiling method, in which the nozzle is strictly perpendicular to the build plate, the 'orientation style' extrusion in our approach puts the extruder tip inside the existing wireframe in most of situations. Hence, collision possibility has to be evaluated carefully for every single stroke. After many experiments, when the extruder nozzle extrudes along the direction of each polygon edge mesh, the cone volume, defined by angle θ (Figure 8), provides a partial solution to avoid the obstacles during extrusion.

To compute the complete fabrication sequence, the first step is to consider how to choose the next strut to print at each state. Assume we have already printed *k* struts, which form sub-structure S_k. Now we have to find an optimal strut with minimal cost to use for subsequent printing. We construct a candidate set of eligible struts for the current decision state, where each eligible strut s in the set satisfies:

- *s* is connected to the current printed structure.
- There are collision-free extruder orientations eligible for the printing *s*.

There might be several eligible struts in the candidate set. We then introduce cost evaluation for each candidate to help us select the most appropriate one. The sequence-searching algorithm 2 (Figure 13) is a kind of searching strategy with quick pruning, using the evaluated cost as a guide, to quickly prune off unnecessary items to avoid searching an unnecessary printing sequence.

Overall algorithm

The re-composition is also considered as a reconstruction of an architectural framework. Each sub-entity contains a structure-like framework by means of its triangle formation. A C++ program was chosen to work with Grasshopper in the Rhinoceros environment. A genetic algorithm, one type of Heuristic algorithm, is employed in this case for a suitable solution to the decomposition and re-organization. (Latombe 2012; Choset 2005). A similar algorithm is applied in the fabrication sequence finding as well.

However, more collision free zones are defined through study of the kinetic features of the industrial robot. This six axis robot performs in a way similar to human limbs but with a lot more strength and precision. Through calculation, there are multiple angles free from collision, but there are only a few candidates that are collision free and compatible with the next strokes. So the algorithm of sequence design attempts to optimize not only the next single struts, but the rest of its group. After tapping all related information into the algorithm (Figure 14), the result is quite unexpected. The optimal sequence is not a continuous polyline-making motion, but a discrete order. In Figure 15, the struts are color coded from yellow to orange according to their

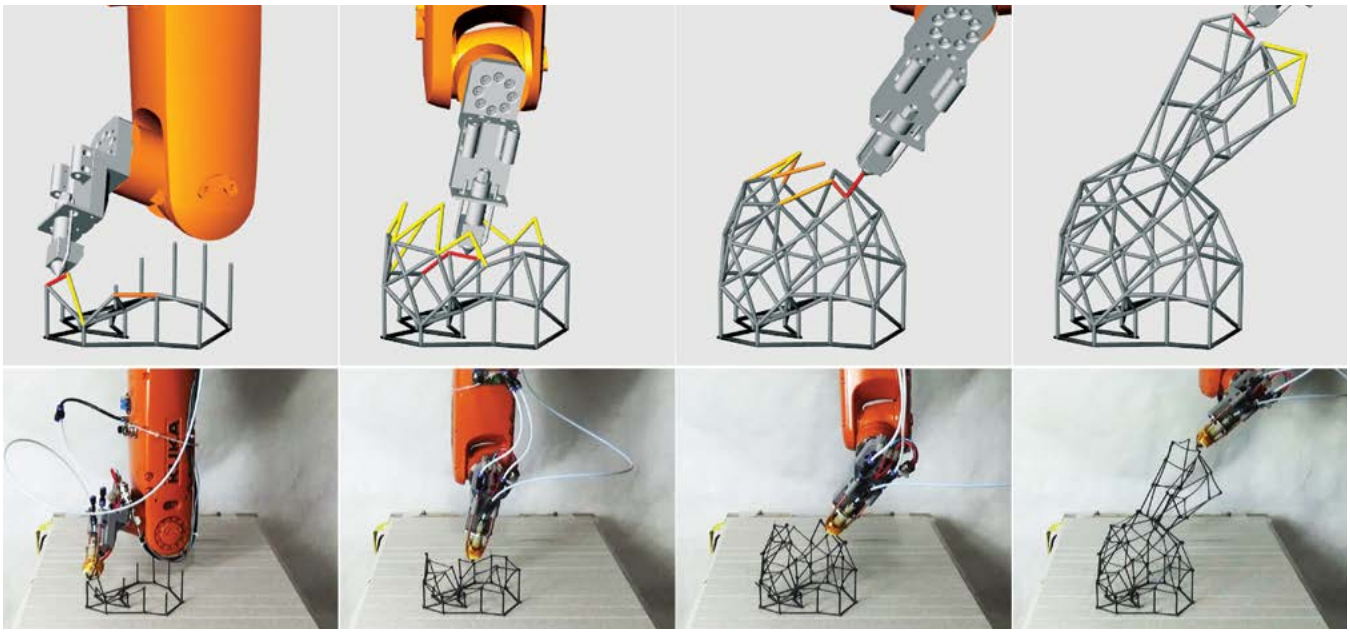

16 Validation Between Virtual Simulation and Physical Fabrication.

order in the construction sequence. The yellow struts have more priority than the orange. In the optimal sequence, the extruder will generate the struts with similar spatial directions first. Then the robot changes its gesture to work on another direction to close the polygon mesh. During the construction process, there are lots of transitional moments that the robot turns its axis drastically from one gesture to another. These transitions actually permit the machine to 3D print in a fluent sequence by skipping any cessation caused by the robot's over-range and singularities.

Spatial Printing Material

Almost all of the spatial thermoplastic extrusion projects confront the same trouble: shrinkage. In the multi-threaded extrusion project, the outer nozzles have to swing a little more toward the center tip to allow all four threads to run into each other. This is because ABS thread has a certain shrinkage during the cooling phase. This phenomenon brings more drawbacks in single-threaded frame printing. Because of shrinkage and self-weight, the single standalone strut which does not have any support from adjacent elements, will have physical deviation causing the end point to lose its position for the next member to pick up. Consequentially, the remaining struts will not keep the relay and the end result is a disastrous mess.

Many thermoplastic filaments, such as ABS and PLA, were tested and proven to have similar deviation problems. PLA has a little more advantage over ABS which has a higher melting temperature and longer cooling time. A custom-made PLA mixed with certain amount of carbon powder is applied to fix this problem. As expected, the strut extruded by this composite PLA filament reduces the deviation into an acceptable range.

Robot Control Based on Mathematics

Robots only works in a certain range due to mechanical constraints. If it goes beyond this range, it will self-lock and cause the whole process to halt. There is also a singularity problem that the alignment of 4th axis and 6th axis causes robot to behave in an unpredictable manner, followed again by an immediate halt. It means that the sets of working sequences figured out from the sequence design have to be re-selected to avoid these issues. KUKA|prc, a Grasshopper plug-in used for generating KUKA robot code, is taken into consideration in this phase. KUKA|prc simulates the whole printing process in Rhinoceros and eliminate the bad key frames, and helps to pipe out the final robotic G-code.

The custom-made extruder is installed on the robot's 6th axis plate. To reduce the extruder's size, a stepper motor is installed on the top of the 4th axis. This extruder design takes the reference of a Bowden extruder, which is popularly used in a lot of desktop 3D printers In this way, the robot effector is lighter and has less interference with other elements. The effector's length and tip angle also heavily influence the validation phase, which has been improved many times based on both calculation and mechanical optimization (Figure 16).

Final Spatial Printing

The Stanford Bunny mesh model was reduced to 179 edges. It

17

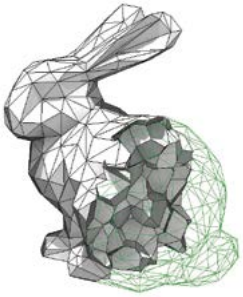

18

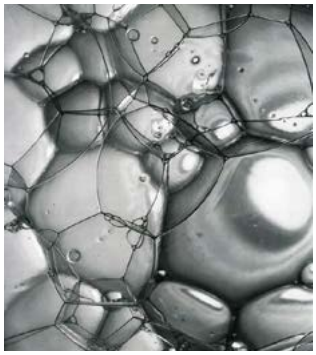

19

17 Concrete Cement Spray on Metal Wireframe.

18 Voronoi Tessellated 3D Polygon Mesh of Stanford Bunny.

19 Soap Bubbles, New York, 1945-6 by Berenice Abbott.

took 14.09 seconds to finish the calculation of mesh decomposition (section 2.3), 36.61 seconds for sequence searching (section 2.4) with a powerful CPU working at 4G frequency. The overall printing time was 91 minutes for a model that is 371 mm in height. However, it took almost one hour to calculate the valid robot working path which was free of collision and self-lock; this was because there were interpreting processes between Rhino and C++, and the most time was wasted in the middle of transition. Since the whole process was validated through computer simulation, the physical printing process was non-stop. All edges were joined together in good condition, especially in the ears area, which is the most difficult part with large overhangs (Figure 20).

CONCLUSION

The method to generate a physical wireframe model based on FDM and robotic technology involved in this paper is divided into two consecutive stages based on different strategies and applications. The latter strategy would have significant potential on the rapid industrial fabrication of large scale building components. The involvement of robotic technology allows architects to gain more control on the fabrication of spatial structures through utilizing mathematical algorithms. The spatial printing methodology based on the original mesh's topological logic confronts many technological challenges on one hand. On the other hand, it is genuinely superior to the layering method of fabrication. Thus this research proposed a novel direction in the field of robotic spatial printing. This direction distinguishes itself from its predecessor in ways such as its geometrical optimization is embedded with many conditions of robotic control, and the process itself involves an intensive amount of complicated data collection and filtration.

However, the current method of thermal melting extrusion places heavy restrictions on the physical quality of the printable materials. This is also the bottleneck of the 3D printing industry on the whole. Only with more adequate materials, can robotic 3D printing technology be transformed into a more adaptable fabrication method that could be wildly applied in the architecture industry.

FUTURE DEVELOPMENT

This research is still currently restricted to a lab environment. A desktop level 3D printer extruder was modified and installed onto a desktop level industrial robot (KUKA KR10 R1100). Thus the operation volume of the machine limits the ability to make architecture components in 1:1 scale. In the upcoming stage we will adopt a heavy-load industrial robot with professional heat melting glue gun, such as a BAK heat gun, installed for fabrication and installation in an architectural dimension.

The Stanford Bunny serves only as a test prototype at this stage. Next, we will adapt this process to the fabrication of complicated surfaces and use reinforced fiber concrete spray casting techniques (Figure 17) for fabricating a series of composite products. We are also aiming to complete a 'solid' mesh (Figure 18&19) with an internal cellular structure after optimizing the algorithms for calculation of robotic motion path, and print a truly spatial physical mesh mold.

REFERENCES

Boyd Stephen, Neal Parikh, Eric Chu, et al. "Distributed optimization and statistical learning via the alternating direction method of multipliers." *Foundations and Trends in Machine Learning*. 3(1): 1–122.

Choset, Howie; Kevin M. Lynch, Seth Hutchinson, George A. Kantor, Wolfram Burgard, Lydia E. Kavraki and Sebastian Thrun. 2005. *Principles of Robot Motion: Theory, Algorithms, and Implementation*. Cambridge: MIT press.

Hack, Norman; Willi Viktor Lauer, Fabio Gramazio and Matthias Kohler. 2014. "Mesh Mould: Differentiation for Enhanced Performance".. Kyoto: CAADRIA. 139–148

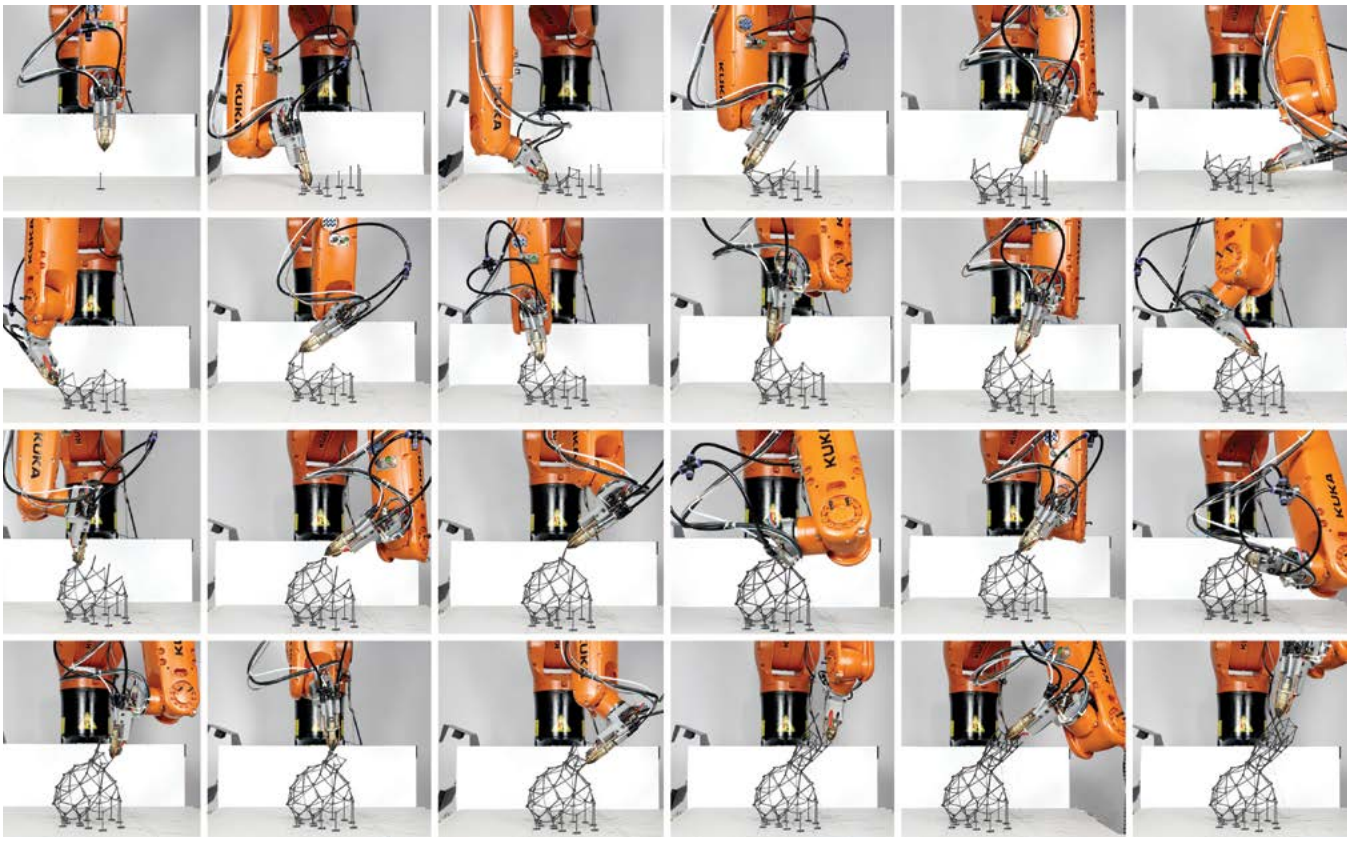

20 Entire Process of 3D Robotic Spatial Printing.

Hughes T J R. 2012. *The Finite Element Method: Linear Static and Dynamic Finite Element Analysis.* Mineola: Dover Publications.

Helm, Volker; Jan Willmann, Andreas Thoma, Luka Piškorec, Norman Hack, Fabio Gramazio, and Matthias Kohler 2015. "Iridescence print: Robotically printed lightweight mesh structures." *3D Printing and Additive Manufacturing* 2(3): 117–122.

Lai, Ming-Jun; Yangyang Xu, And Wotao Yin. "Improved Iteratively Reweighted Least Squares for Unconstrained Smoothed l_q Minimization." *SIAM Journal on Numerical Analysis.*51(2): 927–957.

Latombe, Jean-Claude. 2012. *Robot motion planning*. New York: Springer Science & Business Media.

Kassimali Aslam. 2012. *Matrix Analysis of Structures SI Version.* Indenpendence, KY: Cengage Learning.

Oxman, Neri; Jared Laucks, Marcus Kayser, Elizabeth Tsai, and Michal Firstenberg. "Freeform 3d printing: Towards a sustainable approach to additive manufacturing." *Green Design, Materials and Manufacturing Processes*. Edited by H. Bartolo et. al. London: Taylor & Francis. 479–484.

IMAGE CREDITS

Figures 1, 8, 9, 17, 20: Lei Yu, 2016
Figure 2: Norman Hack, Willi Viktor Lauer, Fabio Gramazio and Matthias Kohler, 2014
Figures 3, 4, 5, 6, 7, 8,: Lei Yu, 2014
Figures 10, 16: Yijiang Huang, Lei Yu, 2016
Figure 11, 12, 13, 14, 15: Yijiang Huang, 2016
Figure 18: Ligang Liu, Lei Yu, 2016
Figure 19: Bernice Abbott, New York, 1945–6

Lei Yu is a Ph.D Candidate, School of Architecture, Tsinghua University. He got the MArch degree from GSD Harvard in 2004. He is the founder of Archi-solution Workshop (ASW,Beijing) , the co-founder of Laboratory for Creative Design (LCD, Beijing), and the co-founder of DADA (Digital Architecture Design Association). His teaching experience includes ETH Zurich, Tsinghua University, and Tongji University. He was featured as Beijing Design Week Elite of 2015.